Mode structure of coupled L3 photonic crystal cavities

A. R. A. Chalcraft,[1] S. Lam,[1] B. D. Jones,[1] D. Szymanski,[1,2] R. Oulton,[1,3] A. C. T. Thijssen[3], M. S. Skolnick,[1] D. M. Whittaker,[1] T. F. Krauss,[2] and A. M. Fox[1,*]

[1]*Department of Physics and Astronomy, University of Sheffield, S3 7RH, UK*
[2]*School of Physics and Astronomy, University of St Andrews, Fife, KY16 9SS, UK*
[3]*Centre for Quantum Photonics, Schools of Physics and Merchant Venturers' School of Engineering, University of Bristol, BS8 1FD, UK*

[*] *mark.fox@sheffield.ac.uk*

Abstract: We investigate the energy splitting, quality factor and polarization of the fundamental modes of coupled L3 photonic crystal cavities. Four different geometries are evaluated theoretically, before experimentally investigating coupling in a direction at 30° to the line of the cavities. In this geometry, a smooth variation of the energy splitting with the cavity separation is predicted and observed, together with significant differences between the polarizations of the bonding and anti-bonding states. The controlled splitting of the coupled states is potentially useful for applications that require simultaneous resonant enhancement of two transitions.

OCIS codes: (230.4555) Coupled resonators; (230.5298) Photonic crystals; (230.5590) Quantum-well, -wire and -dot devices.

References and links

1. Y. Akahane, T. Asano, B. S. Song, and S. Noda, "High-Q photonic nanocavity in a two-dimensional photonic crystal," Nature (London) **425**, 944–947 (2003)
2. S. V. Boriskina, "Photonic molecules and spectral engineering," in *Photonic microresonator research and applications*, I. Chremmos, O. Schwelb, and N. Uzonoglu, eds. (Springer, New York, 2010), pp 393–421.
3. T. D. Happ, M. Kamp, A. Forchel, A. V. Bazhenov, I. I. Tartakovskii, A. Gorbunov, V. D. Kulakovskii, "Coupling of point-defect microcavities in two-dimensional photonic-crystal slabs," J. Opt. Soc. Am. B **20**, 373–378 (2003).
4. S. Ishii, K. Nozaki and T. Baba, "Photonic Molecules in Photonic Crystals," Jap. J. Appl. Phys. **45**, 6108–6111 (2006).
5. D. O'Brien, M. D. Settle, T. Karle, A. Michaeli, M. Salib, and T. F. Krauss, "Coupled photonic crystal heterostructure nanocavities," Opt. Express **15**, 1228–1233 (2007)
6. K. Atlasov, K. F. Karlsson, A. Rudra, B. Dwir, E. Kapon, "Wavelength and loss splitting in directly coupled photonic-crystal defect microcavities," Opt. Express **16**, 16255–16264 (2008)
7. S. Vignolini, F. Intonit, M. Zani, F. Riboli, D. S. Wiersma, L. H. Li, L. Balet, M. Francardi, A. Gerardino, A. Fiore, M. Gurioli, "Near-field imaging of coupled photonic-crystal microcavities," Appl. Phys. Lett. **94**, 151103 (2009).
8. M. Benyoucef, S. Kiravittaya, Y. F. Mei, A. Rastelli, and O. G. Schmidt, "Strongly coupled semiconductor microcavities: A route to couple artificial atoms over micrometric distances," Phys. Rev. B **77**, 035108 (2008).
9. H. Lin, J.-H. Chen, S.-S. Chao, M.-C. Lo, S.-D. Lin, and W.-H. Chang, "Strong coupling of different cavity modes in photonic molecules formed by two adjacent microdisk microcavities," Opt. Express **18**, 23948–23956 (2010).
10. B. M. Möller, U. Woggon, M. V. Artemyev, and R. Wannemacher, "Photonic molecules doped with semiconductor nanocrystals," Phys. Rev. B **70**, 115323 (2004).
11. A. Dousse, J. Suffczynski, O. Krebs, A. Beveratos, A. Lemaitre, I. Sagnes, J. Bloch, P. Voisin, P. Senellart, "Ultrabright source of entangled photon pairs," Nature **466**, 217–220 (2010)

#140134 - $15.00 USD Received 23 Dec 2010; revised 25 Feb 2011; accepted 25 Feb 2011; published 11 Mar 2011

12. A. Dousse, J. Suffczyński, A. Beveratos, O. Krebs, A. Lemaître, I. Sagnes, J. Bloch, P. Voisin, and P. Senellart, "A quantum dot based bright source of entangled photon pairs operating at 53 K," Appl. Phys. Lett. **97**, 081104 (2010).
13. J. Cho, D. G. Angelakis, and S. Bose, "Heralded generation of entanglement with coupled cavities," Phys. Rev. A **78**, 022323 (2008).
14. D. Gerace, H. E. Tűreci, A. Imamoğlu, V. Giovanetti, R. Fazio, "The quantum-optical Josephson interferometer," Nature Phys. **5**, 281–284 (2009).
15. D. M. Whittaker, I. S. Culshaw, V. N. Astratov, and M. S. Skolnick, "Photonic band structure of patterned waveguides with dielectric and metallic cladding," Phys. Rev. B **65**, 073102 (2002).
16. L. C. Andreani, and M. Agio, "Photonic bands and gap maps in a photonic crystal slab," IEEE J. Quantum Electron. **38**, 891–898 (2002).
17. L. C. Andreani, and D. Gerace, "Photonic-crystal slabs with a triangular lattice of triangular holes investigated using a guided-mode expansion method," Phys. Rev. B **73**, 235114 (2006).
18. A. R. A. Chalcraft, S. Lam, D. O'Brien, T. F. Krauss, M. Sahin, D. Szymanski, D. Sanvitto, R. Oulton, M. S. Skolnick, A. M. Fox, D. M. Whittaker, H.-Y. Liu and M. Hopkinson, "Mode structure of the L3 photonic crystal cavity," Appl. Phys. Lett. **90**, 241117 (2007).
19. The modal volumes are similar for B and AB modes, and vary by less than 10% over the range of separations considered. For example, at smallest separation, the B and AB values are $1.64(\lambda/n)^3$ and $1.77(\lambda/n)^3$ respectively. This compares with $V = 0.76(\lambda/n)^3$ for an isolated cavity in the same lattice.
20. Three other modes exist between the $\left[{}^{+}_{-}1\right]$ and $\left[{}^{-}_{-}2\right]$ modes. Unfortunately, the close spacings and low quality factors of these other modes [18] make it impractical to identify their peaks unambiguosly in Fig. 3. It is, however, likely that the predicted 1.5 meV splitting of the $\left[{}^{+}_{+}1\right]$ mode is responsible for the most prominent features; the predicted splittings of the other two modes are insufficient to explain the peak around 1.32 eV.
21. Note that the results for the FDTD simluations become inaccurate for the largest cavity separation, since the intensity above the center of the double cavity becomes very low.
22. E. Gallardo, L. J. Martínez, A. K. Nowak, H. P. van der Meulen, J. M. Calleja, C. Tejedor, I. Prieto, D. Granados, A. G. Taboada, J. M. García, and P. A. Postigo, "Emission polarization control in semiconductor quantum dots coupled to a photonic crystal microcavity," Opt. Express **18**, 13301–13308 (2010).

1. Introduction

The 'L3' defect was the first type of photonic crystal (PhC) nanocavity in which quality (Q) factors in excess of 10^4 were obtained experimentally [1]. This nanocavity consists of a PhC membrane with a line of three holes missed out of a hexagonal lattice. High Q factors are obtained by displacing the end holes slightly outwards, which reduces the radiation losses compared to cavities with undisplaced holes.

In this article, we investigate coupled L3 cavities, which are a class of 'photonic molecules' [2]. An interesting feature of photonic molecules based on coupled PhC cavities [3]–[7] compared to coupled microdisks [8, 9], microspheres [10] or micropillars [11, 12] is that they offer considerable design flexibility as regards their geometry. For example, an L3 photonic molecule can have a number of different orientations, including (see Fig. 1): end-to-end [6], side-to-side, 30° diagonal, and 60° diagonal. As we shall show here, this permits controlled tuning of the energy splitting, which could potentially be used for simultaneous resonant enhancement of two transitions [11, 12]. Moreover, the coupling can also be used to enhance the Q and rotate the polarization, thus offering additional possibilities for detailed mode design. In the long term, this mode control could be important for generating quantum entanglement [13] or implementing quantum-optical Josephson interferometers [14].

The paper is organized as follows. We begin by presenting numerical results for four different geometries. These simulations indicate that the 30° diagonal geometry offers the smoothest control of the mode splitting, and so in Section 3 we present an experimental study of coupled cavities with this orientation. The conclusions are presented in Section 4.

2. Theoretical study

Figure 1 shows the calculated energies and quality factors of the split fundamental modes of parallel L3 cavities coupled along directions at 0°, 30°, 60° and 90° to the line of the defects.

#140134 - $15.00 USD Received 23 Dec 2010; revised 25 Feb 2011; accepted 25 Feb 2011; published 11 Mar 2011

The results were obtained by a guided mode expansion (GME) method derived from refs [15]–[17] for GaAs structures with lattice constant $a = 270$nm, depth $d = 130$nm, fill factor $f = 0.29$ and end-hole displacement $s = 0.15a$. Figure 2 shows the calculated E_x and E_y field profiles for the 30° geometry. (The x and y directions are defined in the inset to Fig. 3.) Since some geometries preclude labelling by strict symmetry, and the E_y field is the dominant component for the fundamental mode of isolated cavities, we term coupled modes with E_y fields of the same sign at each cavity center as bonding (B), and those with E_y fields of opposing signs as anti-bonding (AB). (See Figs 2c and f, respectively.)

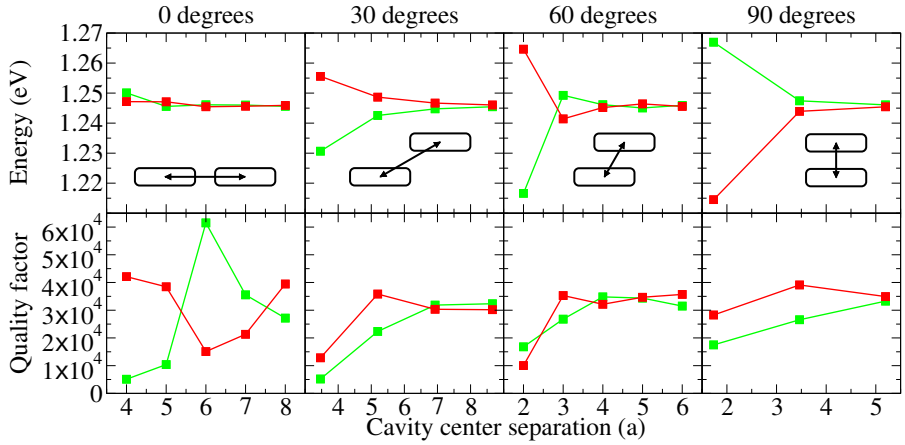

Fig. 1. Theoretical plots of the energies and quality factors of the split fundamental modes of parallel L3 cavities coupled along lines defined relative to those of the cavities. Green lines represent bonding (B) states, red lines represent anti-bonding (AB) states.

It is apparent from Fig. 1 that the mode splitting depends strongly on the coupling geometry. For cavities coupled at 30°, the AB mode consistently has the higher energy, while the opposite is true for the 90° (side-to-side) geometry. However, the energy ordering switches several times for the 0° (end-to-end) and 60° geometries, due to oscillations in the coupling matrix element. Larger energy splittings for minimal separations are achieved from cavities coupled at greater angles, since these geometries allow greater proportions of the cavities to be in close proximity. Thus the largest splitting is calculated for the 90° geometry. However, the splitting drops off very rapidly with separation, in contrast to the 30° geometry, which provides the smoothest variation in the inter-cavity coupling due to the field extension along the 30° direction. For this reason, the experimental study in Section 3 focuses on the 30° geometry.

The high Q factor of the fundamental mode of isolated L3 cavities is caused by the suppression of the radiation losses. The E_x field component has odd parity about both the x and y axes, which automatically causes field cancellation in the forward direction. This is not true for the even-parity E_y component, and the high Q is caused by minimizing the integrated in-plane E_y field by fine tuning of the end hole positions [18]. The equivalent optimization for coupled cavities is complicated by the different relative signs for the B and AB mode fields within the two cavities. The fields at the cavity centers have opposite polarities in the AB mode, which makes cancellation of radiation in the forward direction possible. This is not the case for the B mode, and so we would, in general, expect the AB mode to have the higher Q.

The theoretical Q factors presented in Fig. 1 confirm that the AB mode does usually have the higher Q, although there are notable exceptions, especially in the 0° geometry. This particular geometry is further complicated by the fact that, at minimal separation, the single hole

#140134 - $15.00 USD Received 23 Dec 2010; revised 25 Feb 2011; accepted 25 Feb 2011; published 11 Mar 2011

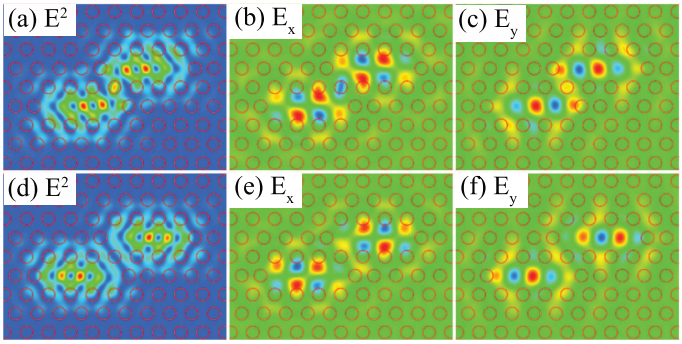

Fig. 2. Theoretical in-plane electric fields at the center of the slab for the bonding (a-c) and anti-bonding (d-f) states. (a,d) $|\mathbf{E}|^2$; (b,e) $\mathbf{E}_x$; (c,f) $\mathbf{E}_y$. Color scales run from blue (low) to red (high). In (a) and (d), blue and red represent zero and high intensity respectively, while in (b), (c), (e) and (f), blue is negative and red positive.

separating the two cavities cannot be displaced in two directions at the same time. The calculations were thus performed with the hole undisplaced, and this results in a very large difference between the B and AB modes. It is particularly noteworthy that the Q of the B mode is significantly higher than that of the isolated cavities ($\approx 40,000$) at a cavity separation of $6a$. The use of coupled cavities can thus lead to an enhancement of Q, although at the expense of a larger modal volume V, such that Q/V is not enhanced [19].

In the 30° geometry, the perturbation of the cavities' fields due to the coupling results in low Q factors for minimal separation, with the AB mode having the larger Q at small separations. This contrasts with the 60° geometry, where the AB mode has the lower Q at the minimal separation on account of anomalously strong coupling to lossy states at the edge of the light cone. In the 90° geometry, the AB mode consistently has the higher Q factor, as expected.

3. Experimental study

The theoretical studies in Section 2 indicate that the 30° geometry offers the smoothest control of the coupling. L3 photonic molecules with this geometry were therefore fabricated by electron beam lithography in a GaAs membrane containing a single layer of InAs quantum dots with a density of $\sim 5\times10^{10}$ cm^{-2}. ZEP520A resist was exposed with a dose of $36\,\mu$C cm^{-2} at 30 kV, and the pattern was transferred into the GaAs by Cl_2-based chemically assisted ion beam etching (CAIBE). Air-bridges were then formed by selective etching with buffered hydrofluoric acid of a $1\,\mu$m-thick sacrificial $Al_{0.6}Ga_{0.4}As$ layer. Photonic molecules were prepared with one, two, three, or four holes between the cavities, corresponding to separations from $2\sqrt{3}a$ to $5\sqrt{3}a$, with the same d, a, f and s parameters as in Section 2. A scanning electron microscope image of a typical sample is included in Fig 3. Photoluminescence (PL) measurements were made by using the dots as an internal light source under 633 nm excitation from a HeNe laser. The light was collected in the direction normal to the sample surface through a microscope objective with a numerical aperture of 0.42. The samples were mounted in a helium flow cryostat, at a temperature of ~ 10 K.

Figure 3 compares a spectrum from an isolated cavity to that of dual cavities with the minimum spacing of $2\sqrt{3}a$. The modes are labelled according to the in-plane parities of their E_x fields at the center of the membrane, following the notation defined in ref. [18]. We place the parity along the x axis above the parity along the y axis, and add a numerical index denoting their ordering in terms of energy. In the coupled cavities, clear splittings are observed for sev-

#140134 - $15.00 USD Received 23 Dec 2010; revised 25 Feb 2011; accepted 25 Feb 2011; published 11 Mar 2011

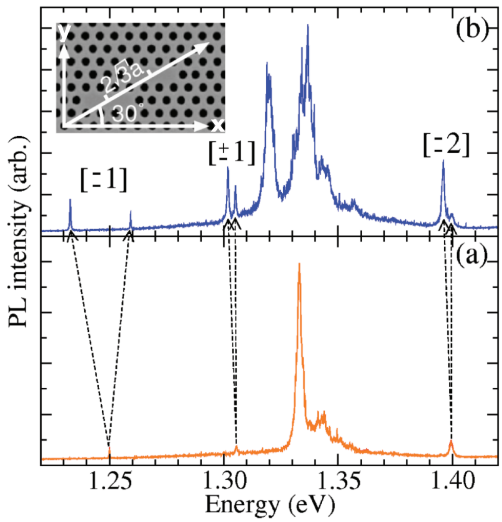

Fig. 3. Comparison of an experimental PL spectrum from (a) an isolated cavity, and (b) a photonic molecule with a pair of cavities separated by $2\sqrt{3}a$. The inset shows the experimental geometry with 30° diagonal coupling.

eral modes. The largest splitting of 26 meV was observed for the fundamental, $[-1]$, mode. The splittings of the $[\mp 1]$ and $[-2]$ modes were respectively 3.3 meV and 2.2 meV [20]. The weaker coupling of these higher-order modes may be understood qualitatively in terms of their field patterns. The field of the fundamental mode of an individual L3 cavity spreads out along the 30° direction, facilitating strong inter-cavity coupling, but the $[\mp 1]$ and $[-2]$ modes are much more tightly localized in that direction.

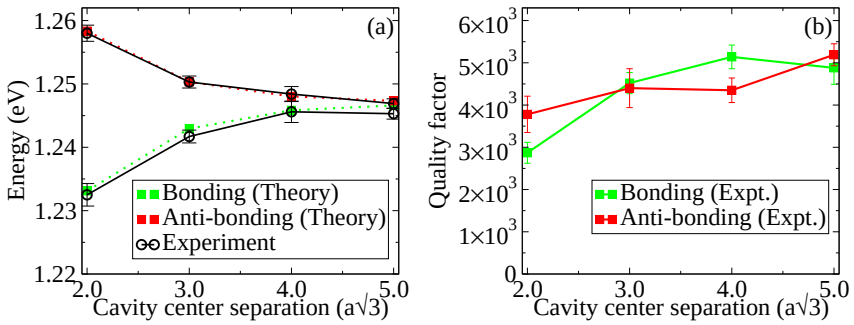

Fig. 4. Energies (a) and quality factors (b) of the split fundamental modes of coupled L3 cavities in the 30° geometry. The theoretical results for the modes energies from Section 2 are included for comparison in (a).

The splitting of the fundamental mode is explored in more detail in Fig. 4(a), with the error bars representing the standard deviation for ten pairs of cavities. The experimental mode energies demonstrate excellent agreement with the theoretical results. The experimental Q factors shown in Fig. 4(b) are lower than the theoretical ones given in Fig. 1 on account of losses due to imperfect fabrication and/or background absorption. Nevertheless, the predicted reduction in Q for the minimally-spaced cavities is observed in the data. This reduction is a consequence of the perturbation to the optimized fields of the individual L3 cavities caused by the coupling.

#140134 - $15.00 USD Received 23 Dec 2010; revised 25 Feb 2011; accepted 25 Feb 2011; published 11 Mar 2011

The two modes also differ in their polarization. Figure 5 shows the average experimental polarization angles (solid circles) of the fundamental modes in the 30° geometry as a function of cavity separation. The results were obtained by measuring the intensity as a function of linear polarizer angle in detection. The inset shows a polar plot of the mode intensities for the $2\sqrt{3}a$ separation, where 0° corresponds to the x axis (i.e. parallel to the L3 cavity long-axis) and 90° to the y axis (i.e. perpendicular to the L3 cavity axis). The main figure shows the polarization angle of each mode, determined as the axis of maximum intensity from the polar plots, as in the inset. The fundamental modes of isolated L3 cavities are polarized along the y axis due to the parities of their in-plane electric field components [18]. It is therefore unsurprising that the modes of weakly-coupled pairs of cavities exhibit polarizations that lie very close to the y axis. However, as we reduce the cavity separation, the field distributions become more strongly perturbed, and the B mode gradually rotates. For the cavities with the smallest separations, the polarization of the B mode is approximately orthogonal to the coupling axis.

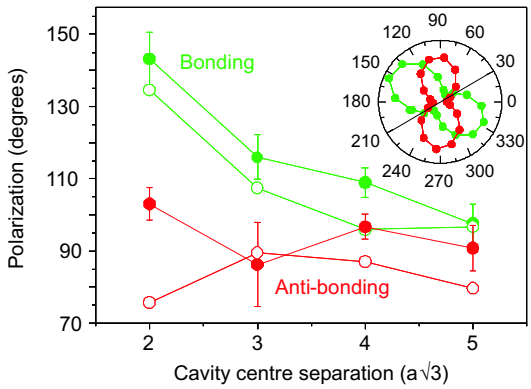

Fig. 5. Experimental (solid circles) and theoretical (open circles) polarization angles for the 30° geometry as a function of cavity separation. The inset shows the polar plot for a cavity separation of $2\sqrt{3}a$. The line at 30° indicates the coupling axis.

The open circles in Fig. 5 show finite difference time domain (FDTD) simulations of the polarization 1μm above the cavity at a point in the center [21]. The experimental trends are reproduced, although the quantitative agreement is not perfect. The discrepancies may indicate that the polarization is very sensitive to perturbations in the barrier associated with fabrication errors. Overall, the results in Fig. 5 show that coupled cavities may be used to engineer the mode polarization, which is an important consideration when coupling QDs to cavities [22].

4. Conclusions

We have performed numerical simulations of coupled L3 PhC cavities in four different geometries, and have found that the 30° geometry shows the smoothest variation in the energy splitting of the fundamental mode with respect to cavity separation. Experimental results for this geometry are in excellent agreement with the simulations. Significant differences were observed for the polarization of the bonding and anti-bonding states, again in agreement with theory. Our results should facilitate informed decisions over the suitability of various geometries for different applications, for example, for double photonic resonances in quantum dots.

Acknowledgments

This research was supported by the EPSRC through the QIPIRC and grants GR/S76076/01 and EP/G001642/1.

#140134 - $15.00 USD Received 23 Dec 2010; revised 25 Feb 2011; accepted 25 Feb 2011; published 11 Mar 2011